RSC Sustainability

ROYAL SOCIETY OF CHEMISTRY

PAPER

View Article Online
View Journal | View Issue

Cite this: *RSC Sustainability*, 2025, **3**, 4020

Oxyethylene-substituted bis-indolyl derivatives for enhanced cyanide detection: mechanistic insights and application in food safety analysis†

Nilanjan Dey, ‡[a] Subham Bhattacharjee,‡[b] Namita Kumari[c] and Santanu Bhattacharya *[cd]

Received 1st December 2024
Accepted 30th April 2025

DOI: 10.1039/d4su00756e

rsc.li/rscsus

In this study, we synthesized highly colored, oxidized bis-indolyl derivatives featuring oligo oxyethylene chains on the central phenyl ring, significantly enhancing the solubility of the probe molecule in water. This improved solubility enabled a pronounced response to cyanide ions, facilitating naked-eye detection *via* a color-changing response and a turn-on fluorescence response (detection limit of ~17 ppb). Mechanistic investigations revealed a time-dependent, two-step interaction with cyanide. Initially, hydrogen bonding or deprotonation of the indolyl-NH protons by cyanide caused an immediate color change from red to yellow. Over time, a Michael addition reaction triggered by cyanide further altered the color of the solution to colorless, disrupting the conjugation. The formation of the chemodosimetric adduct was confirmed using ^{1}H NMR, ^{13}C NMR, and mass spectroscopies. The system also successfully detected endogenous cyanide in cassava, both in aqueous extracts and on the vegetable surface (without any pretreatment). In addition, we evaluated conventional washing techniques for cyanide removal from cassava, highlighting the potential of these oxidized bis-indolyl derivatives for cyanide detection and remediation in crops.

Sustainability spotlight

In addition to the detection of free cyanide in water, the detection of endogenously bound cyanide ions in many food items is crucial. Cassava is a major food for more than 500 million people in Africa, Asia and Latin America. Thus, to determine the utility of the present probe for the detection of endogenously bound cyanide, we used it to detect the presence of cyanide ions in cassava (*Manihot esculenta*). The visual response to cyanide was observed not only in the aqueous extract of the food sample but also when it was directly spiked on the surface. In addition, we examined whether conventional washing techniques can remove cyanide from cassava samples or not. Such studies will be beneficial not only for the detection of endogenous cyanide in crops but also for developing proper remediation techniques.

1. Introduction

Oxidized bisindolyl methane (BIM) compounds often exhibit a strong charge transfer characteristic, leading to noticeable color changes upon interaction with specific analytes, even at trace levels.[1] In addition to ionic analytes, such as toxic anions and heavy metal pollutants, these compounds show high sensitivity towards changes in environmental conditions, such as pH, polarity, and even the ionic strength of the medium.[2] Unlike their unoxidized precursors, the oxidized BIM derivatives are generally stable under ambient conditions, which ensures that the sensor will remain effective over a longer period. The synthesis of BIM derivatives is relatively easy, starting from inexpensive precursors, which makes them attractive for developing low-cost sensors.[3] In addition, oxidized BIM compounds are often found to be biocompatible, making them suitable for applications in biological and clinical settings, such as detecting biomarkers or contaminants in physiological samples (*e.g.*, human urine, sweat, or blood).[4] Despite such advantages, the limited solubility of these probes in aqueous environments often affects the kinetics of the sensing process and hinders their effective interaction with analytes.[5] Also, the susceptibility of BIM derivatives towards the microenvironment sometimes influences the stability of the sensor molecules and their response towards analytes, leading to inconsistent or unreliable results. The other pertinent issue

[a]*Department of Chemistry, Birla Institute of Technology and Science Pilani, Hyderabad 500078, India*

[b]*Department of Chemistry, Kazi Nazrul University, Asansol 713303, West Bengal, India*

[c]*Department of Organic Chemistry, Indian Institute of Science, Bangalore 560012, India. E-mail: sb@iisc.ac.in*

[d]*Department of Chemistry, Indian Institute of Science Education and Research, Tirupati, Andhra Pradesh-517507, India*

† Electronic supplementary information (ESI) available. See DOI: https://doi.org/10.1039/d4su00756e

‡ Both authors contributed equally.

is the limited shelf life of oxidized BIM derivatives, as they can undergo gradual degradation when exposed to air, light, or moisture for extended periods.[6]

Considering these properties, herein, we designed and synthesized oxidized BIM derivatives with two oligo-oxyethylene chains attached to a central phenyl ring. Incorporating oligo-oxyethylene (OEG) chains into sensor molecules offers multiple advantages (Fig. 1). These chains improved the solubility in aqueous environments, enhanced the biocompatibility, and offered anti-fouling properties by resisting non-specific interactions with biomolecules, thereby ensuring high selectivity.[7] Their flexibility aids in better interaction with analytes, facilitating faster response times and improving the sensor performance.[8] Furthermore, OEG chains form a hydrophilic interface, making them suitable for detecting polar analytes. Their exceptional thermal and chemical stability further ensures consistent performance under varying conditions.

As expected, the as-synthesized compound showed significant solubility in an aqueous environment and exhibited a ratiometric, color-changing response towards cyanide ions in water. Notably, acute exposure to cyanide can cause symptoms such as headache, confusion, nausea, difficulty breathing, loss of consciousness, and even death due to cardiac failure. In contrast, chronic low-level exposure may lead to long-term neurological effects, such as weakness, vision impairment, and cognitive deficits. The mechanistic investigation indicated that the hydrogen bonding interaction of indolyl-NH units with cyanide led to an immediate change in the solution color from red to yellow. However, over time, cyanide could attack the electron-deficient meso carbon center and reduce the overall conjugation. This can be attributed to a time-delayed color-changing response from yellow to colorless with cyanide ion. Consequently, we ultimately witnessed a time-dependent sequential chromogenic response with cyanide ions because of two distinct sensing mechanisms: hydrogen bonding followed by chemodosimetric interaction. Considering the highly selective naked eye response towards cyanide ions, the probe was used to detect endogenous cyanide in the staple food cassava. Not only in the aqueous extract, the color-changing response towards cyanide was observed in the freshly chopped vegetable samples without any preprocessing. Interestingly, the loss of cyanide in the conventional washing treatment could be determined in a semi-quantitative manner using the present system.

2. Experimental section

2.1. Materials and methods

All solvents were of analytical grade and were used without further purification. Each chemical used for the synthesis and spectroscopic titration was of the best grade available. ^{1}H-NMR and ^{13}C-NMR spectra were recorded on a Bruker Advance DRX 400 spectrometer operating at 400 and 100 MHz for ^{1}H and ^{13}C NMR spectroscopy (in DMSO-d_6). IR spectra were recorded on a PerkinElmer FT-IR Spectrum BX. UV-vis absorption spectra were obtained on a Shimadzu UV-2100 spectrophotometer. Fluorescence spectra were recorded using a Fluorolog Horiba Jobin Yvon spectrofluorometer. The stock solution of the compound was prepared in dimethyl sulphoxide (DMSO), and the final concentration of DMSO in all the studies was less than 0.5%. The synthetic scheme for compound **1** and the detailed characterization data are presented in Fig. 2.

2.2. Synthesis and characterization

2.2.1. Compound (1). To a solution of 3 (50 mg, 0.109 mmol) and indole (51.5 mg, 0.440 mmol) in dry MeOH, I_2 (5 mg) was added and stirred for 1 h at room temperature. The intermediate was purified by precipitation (3 times) from MeOH. DDQ (2 mmol) was added to a solution of the intermediate compound in dry CH_3CN at room temperature. After overnight reaction, the solvent was removed, and the product was purified by precipitation (3 times) from diethyl ether. Yield 78 mg, 80.8%; IR (Neat, cm^{-1}) 3048.2, 2201.2, 1527.6, 1472.1, 1405.5, 114.7, 746.4, 583.5; ^{1}H NMR (400 MHz, DMSO-d_6) δ 2.90–2.95 (m, 10H), 3.06–3.09 (m, 6H), 3.21–3.26 (m, 9H), 3.64 (t, $J = 4$ Hz, 5H), 7.13–7.18 (m, 8H), 7.34 (t, $J = 4$ Hz, 6H), 7.63 (d, $J = 8$ Hz, 4H), 8.45 (s, 4H); ^{13}C NMR (100 MHz, DMSO-d_6) δ 58.0, 68.4, 69.4, 69.5, 69.7, 71.2, 98.4, 115.7, 116.6, 118.0, 120.7, 123.3, 125.5, 127.6, 131.1, 151.5; HRMS m/z calcd for $C_{54}H_{54}N_4O_8$(M + H)$^+$ 887.4020, found 887.4017.

2.2.2. Dimethyl 2,5-dihydroxybenzene-1,4-dioate (5). Dimethyl 2,5-dioxocyclohexane-1,4-dicarboxylate (5 g, 21.9 mmol.) and NCS (3.0 g, 22.4 mmol.) were placed in a 100 mL round-bottomed flask. To this end, 15 mL of glacial acetic acid was added and heated at 80 °C for 1 h. The reaction mixture was then cooled. The yellow precipitate that appeared due to cooling was filtered and washed with 50 mL of water. The precipitate was dried in air, followed by drying under a vacuum

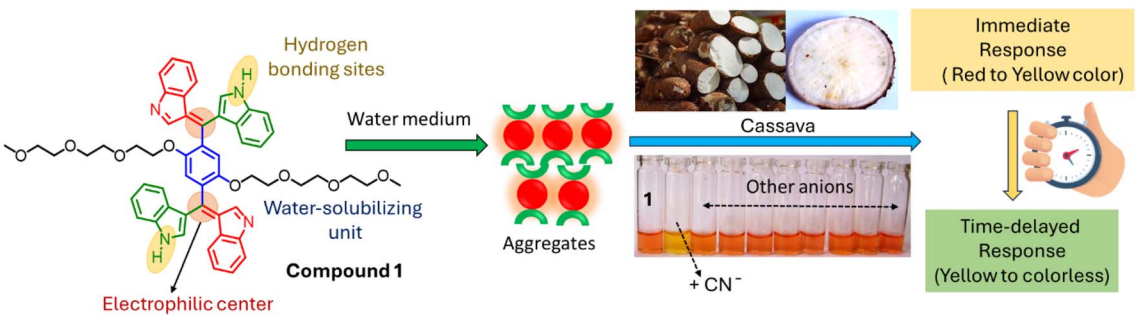

Fig. 1 Chemical structure of compound **1** and schematic showing the time-dependent step-wise cyanide sensing.

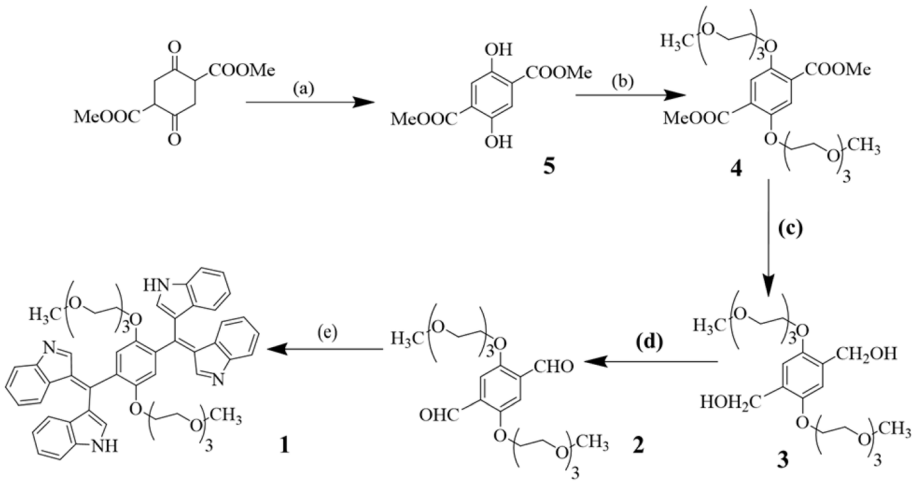

Fig. 2 Synthetic scheme for the design and synthesis of compound **1**. Reagents, conditions and yields: (a) NCS, glacial AcOH, 80 °C, 1 h, 80.8%; (b) K_2CO_3, DMF, 60 °C, 2 h, 68.5%; (c) LAH, dry THF, reflux, 2 h, 80%; (d) PCC, dry DCM, 2 h, 90.8%; (e) indole, I_2, MeOH, rt, 1 h; followed by DDQ, CH_3CN, rt, 1 h, 80.8%.

pump. Yield 4.0 g, 80.8%; mp 175–177 °C; IR (Neat, cm^{-1}) 3275.9, 2958.3, 1831.4, 1646.9, 1491.7, 1430.9, 1331.1, 1197.4, 1019.4, 950.9, 889.7, 788.3; ^{1}H NMR (400 MHz, $CDCl_3$) δ 3.97 (s, 6H), 7.47 (s, 2H), 10.06 (s, 2H).

2.2.3. Bis-ester (4). To a solution of **5** (7 g, 30.97 mmol) in 70 mL of dry DMF, anhydrous K_2CO_3 was added under an N_2 atmosphere and stirred at 60 °C for 30 min. Then, 2-(2-(2-methoxyethoxy)ethoxy)ethyl 4-methylbenzenesulfonate (21.63 g, 68 mmol) was added under an N_2 atmosphere, and the mixture was heated to 60 °C for 2 days. After completion of the reaction, the solvent was removed under reduced pressure. The residue was dissolved in 100 mL of $CHCl_3$ and washed with 1 M NaOH solution (2 × 50 mL), followed by 1 M HCl solution (2 × 50 mL), and then with water (2 × 50 mL). The solution was dried over anhydrous Na_2SO_4 while the solvent was removed. This yielded an oily material, which was purified by chromatography using silica gel hexane/EtOAc (1–2.25% MeOH/$CHCl_3$ as eluant). Yield 11 g, 68.5%; IR (Neat, cm^{-1}) 3208.3, 2877.3, 2681.0, 1725.0, 1618.1, 1496.0, 1411, 1319.9, 1196.9, 1102.7, 1019.7, 751.8, 643.7; ^{1}H NMR (400 MHz, $CDCl_3$) δ 3.38 (s, 6H); 3.55–3.56 (m, 4H), 3.64–3.69 (m, 8H), 3.75–3.78 (m, 4H), 3.87–3.90 (m, 10H), 4.18 (t, J = 3.6 Hz, 4H), 7.42 (s, 2H); HRMS m/z calcd for $C_{24}H_{38}O_{12}$ $(M + Na)^+$ 541.24, found 541.2261.

2.2.4. Bis-alcohol (3). LAH (4.34 g, 114.2 mmol) was carefully added to a solution of **5** (5.74 g, 11.06 mmol) in dry THF at 0 °C under N_2 atmosphere, and the mixture was stirred for 30 minutes at 0 °C. Then, it was refluxed for 2 h, followed by cooling to 0 °C. The excess LAH was quenched with ethyl acetate and then with water. HCl (3 N) was added dropwise to quench all the LiOH formed during the quenching of excess LAH. The product was extracted with $CHCl_3$ repeatedly and the solution was dried over anhydrous Na_2SO_4, followed by rotary evaporation of the solvent a colorless oil: yield 4.1 g, 80%; IR (Neat, cm^{-1}) 3411.5, 2927.8, 2878, 1654.5, 1510.7, 1457.4, 1202.3, 1107.9, 1063.6, 947.6, 662.4; ^{1}H NMR (400 MHz, $CDCl_3$) δ 3.73 (s, 6H), 3.54–3.56 (m, 4H), 3.63–3.67 (m, 8H), 3.70–3.71), (m, 4H), 3.82 (t, J = 4.4 Hz, 4H), 4.18 (t, J = 4.4 Hz, 4H), 4.63 (s, 4H); 6.85 (s, 2H); HRMS m/z calcd for $C_{22}H_{38}O_{10}$ $(M + Na)^+$ 485.25, found 485.2363.

2.2.5. Bis-aldehyde (2). To a solution of **4** (2 g, 4.3 mmol) in 50 mL of dry DCM, PCC (3.73 g, 17.3 mmol) was added at a time. The mixture was stirred for 3 h at room temperature. Purification of the product obtained was carried out by chromatography on a silica gel column (3.5 : 96.5, $CH_3OH/CHCl_3$) to afford a light yellow oil. Yield 1.8 g, 90.8%; ^{1}H NMR (400 MHz, $CDCl_3$) δ 3.37 (s, 6H); 3.54–3.56 (m, 4H), 3.64–3.68 (m, 8H), 3.71–3.74 (m, 4H), 3.88–3.91 (m, 4H), 4.27 (t, J = 4.8 Hz, 4H), 7.46 (s, 2H), 10.52 (s, 2H); HRMS m/z calcd for $C_{22}H_{34}O_{10}$ $(M + Na)^+$ 481.22, found 481.2050.

2.3. Spectroscopic studies

The UV-vis and fluorescence spectra of the compounds with and without anions were recorded on a Shimadzu model 2100 and Cary Eclipse spectrofluorimeter, respectively. For both UV-visible and fluorescence studies, the concentrations of the compounds were fixed at 20 μM. For the emission experiments, the slit widths for both the excitation and emission channels were 5 nm. The excitation wavelength was fixed at 465 nm.

3. Results and discussion

3.1. Optical properties of probe molecule

We synthesized probe **1** by coupling indole with oxyethylene terephthaldehyde, followed by oxidation using DDQ (2, 3-dichloro-5,6-dicyano-1,4-benzoquinone).[9] The sensing properties of the compound were investigated in aqueous medium. The UV-visible spectra of compound **1** in water exhibited two prominent absorption bands at 392 ($\varepsilon = 2.62 \times 10^6$ M^{-1} cm^{-1}) and 510 ($\varepsilon = 3.37 \times 10^6$ M^{-1} cm^{-1}) nm, respectively. The red-shifted charge transfer band at a longer wavelength region

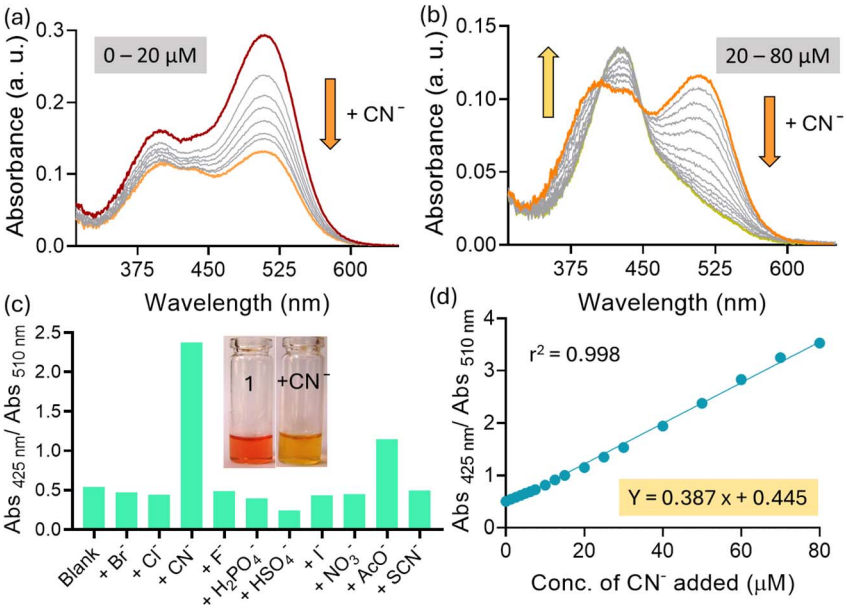

Fig. 3 UV-visible titration of **1** (20 μM) with CN^- in (a) 0–20 μM and (b) 20–80 μM in aqueous medium. (c) Ratiometric changes in the absorbance of **1** upon the addition of various anions (80 μM) in aqueous medium. (d) Ratiometric changes in the absorbance of **1** upon addition of CN^- (0–80 μM) in aqueous medium.

(~510 nm) is attributed to the zwitterionic form of **1**.[10] The color of the solution changed from red to yellow after the addition of cyanide ions. The UV-vis spectra revealed a complete shift of the band from 510 to 431 nm in the presence of cyanide ions in water. The plot of absorbance ratio (425 nm/515 nm) with respect to the added anions showed a selective response toward the cyanide ion (Fig. 3c). The other anions did not show much change even when added in 5 times excess. Although a small change was observed with the acetate ion, the extent was negligible compared with that of cyanide.

3.2. Interaction with cyanide in aqueous medium

The UV-visible titration of probe **1** was then performed using cyanide ions under similar conditions (Fig. S1†). Till 1 equiv. addition of cyanide, the absorbance intensity decreased only at 510 nm (Fig. 3a). However, beyond one equiv., the absorbance at the 427 and 387 nm bands was enhanced at the expense of the absorbance at the 510 nm band (Fig. 3b). The presence of multiple isosbestic points at 404 and 450 nm was noted during the titration studies. This indicates the existence of an

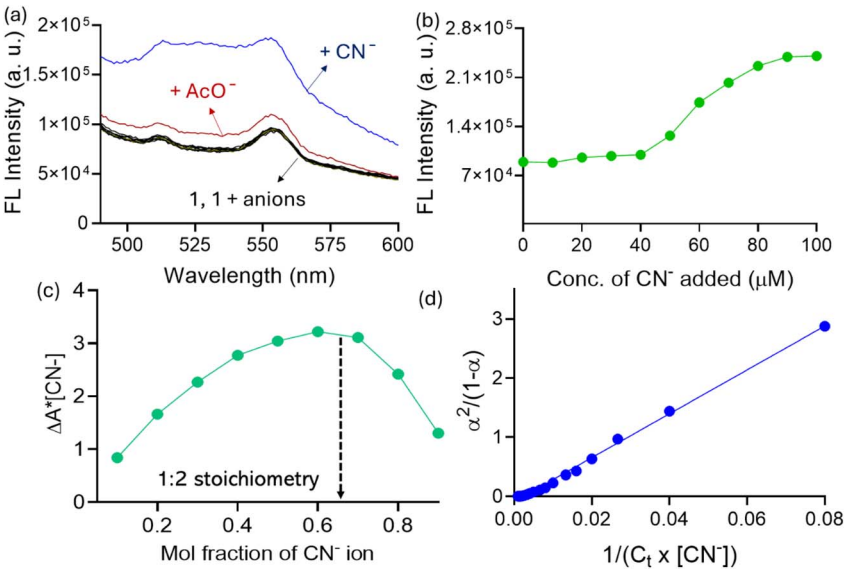

Fig. 4 (a) Fluorescence spectra of **1** (20 μM, $\lambda_{ex} = 465$ nm) with different anions (80 μM) in aqueous medium. (b) Changes in FL intensity of **1** (20 μM, $\lambda_{ex} = 465$ nm) upon addition of CN^- (0–100 μM) in aqueous medium. (c) Job's plot showing stoichiometry of the interaction between **1** and CN^- ion. (d) Determination of the binding constant between **1** and CN^- ion.

equilibrium between the probe and the cyanide ion complex. Furthermore, the absorbance ratios at 510 and 425 nm were plotted against the added cyanide ion concentrations. It provided a straight line with a correlation coefficient of 0.996 (Fig. 3d). This indicates that compound **1** can be used as a ratiometric, naked-eye sensor for detecting cyanide ions in water.

The stoichiometry of the interaction between probe **1** and the cyanide ion was determined to be 1 : 2 based on Job's plot analysis (Fig. 4c). Furthermore, the binding constant of the cyanide ion was estimated to be 10.13 ± 0.01 ($\log K$) using the Benesi–Hildebrand equation for 2 : 1 stoichiometry (Fig. 4d). The detection limit of cyanide ions was calculated using UV-vis spectroscopy. The calibration plot was generated by considering changes in absorbance at the 510 nm band. The 10 blank readings of the probe were considered for calculating the standard deviation, and subsequently, the detection limit was estimated at 16.6 ppb, which is ~13 times less than the permitted limit of cyanide in water. Compound **1** exhibited very faint fluorescence in the aqueous medium. Upon excitation at 465 nm, a small fluorescence band was observed with emission maxima at ~552 nm region. The addition of cyanide ions resulted in ~2.3-fold enhancement of the fluorescence intensity. No other anions except acetate showed any detectable response. Only a slight enhancement of the fluorescence intensity (~4 times less than CN^-) was noted against the acetate ion (Fig. 4a). Therefore, from fluorometric analysis, we can selectively detect cyanide ions in water medium. Furthermore, fluorescence titration studies were performed with cyanide ions. Interestingly, till 1 equiv. of cyanide ion, there was very little change in the fluorescence spectra. However, beyond 1 equiv., the fluorescence intensity was systematically enhanced upon the addition of cyanide ions (Fig. 4b).

3.3. Immediate response of cyanide as a base

Since cyanide can act both as a nucleophile and a base, we have performed a series of spectroscopic studies to comment on the mechanism of cyanide interaction.[11] The UV-visible spectral analysis revealed blue-shifted absorption maxima upon interaction with hydroxide ions (Fig. S2†). A similar observation was noted for cyanide, which indicated the possibility of hydrogen bonding (or deprotonation) interactions with the cyanide ion.

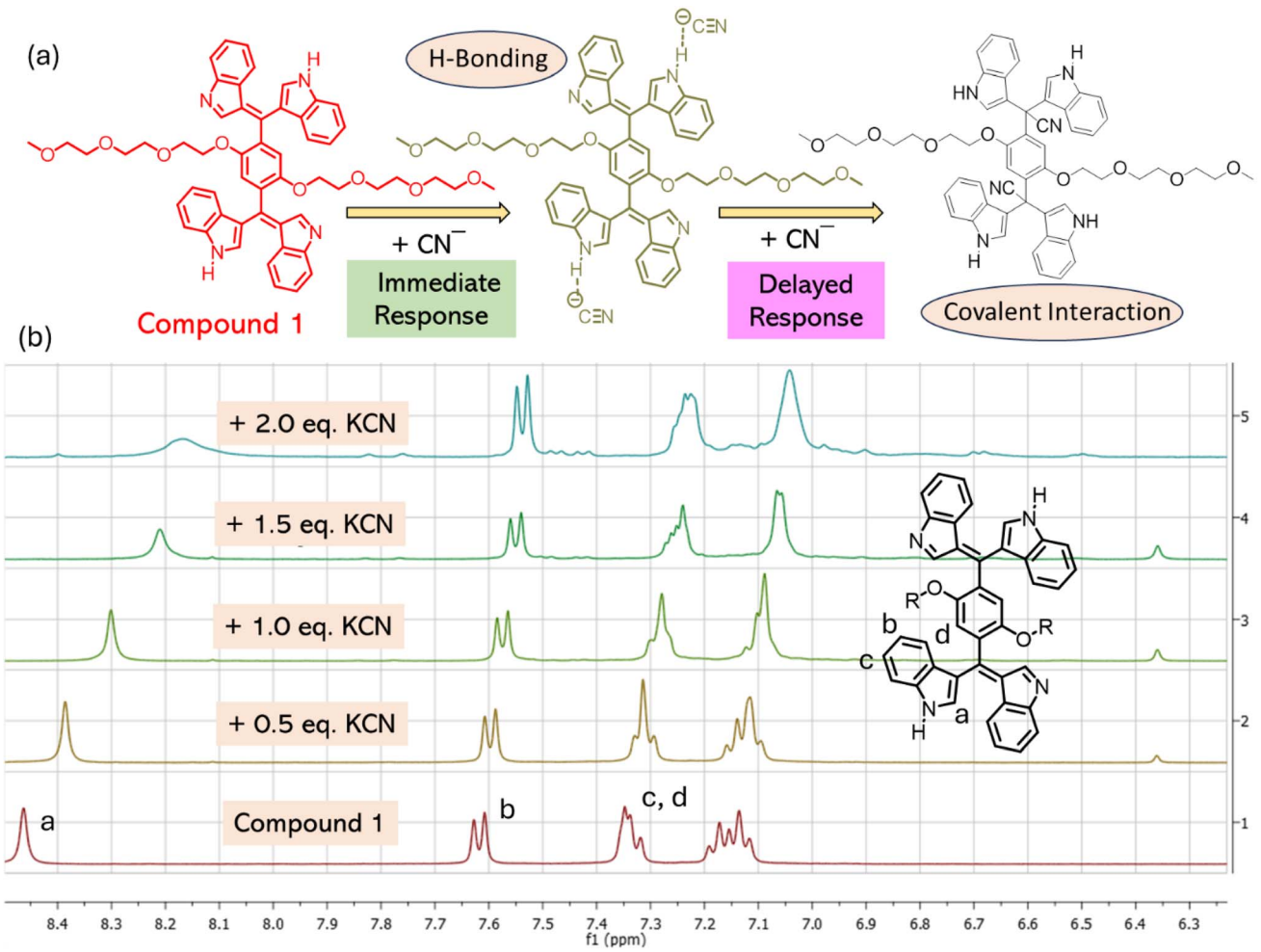

Fig. 5 (a) Schematic showing the time-dependent stepwise interaction of **1** with the CN^- ion. (b) Partial ^{1}H-NMR spectra of **1** (5 mM) with CN^- in DMSO-d_6 medium. [The chemical structure is shown with assigned protons].

In addition, Job's plot showed a 2 : 1 interaction of the cyanide ion, indicating interaction of the CN^- ion with the two indolyl-NH moieties of probe **1**. To validate the above mechanism, ^{1}H-NMR titration of the probe with cyanide ions was carried out in DMSO-d_6 medium (Fig. 5b). Both probes exhibited similar interactions with the cyanide ion. In the presence of cyanide ions, the aromatic protons experienced upfield shifts. Among them, the protons adjacent to indolyl nitrogen centres showed the maximum shift with substantial broadening. This indicated the involvement of indolyl-NH protons in hydrogen bonding interactions with cyanide ions (Fig. 5a).[12]

3.4. Delayed response of cyanide as a nucleophile

Interestingly, when the cyanide-treated solution of compound **1** was kept for more than 2 days under ambient conditions, we observed a change in the color of the solution from yellow to colourless. The UV-visible spectrum showed no major absorption bands in the visible region (Fig. 6a). Rather, the spectrum showed uncanny similarity with the UV-visible spectrum of the unoxidized precursor. This indicated that the CN^- interacted with the probe in a manner that influenced the conjugation of the molecule. In other words, CN^- ion could attack the electron-deficient meso carbon center and cut off the overall conjugation (Fig. 6b).[13] To prove this further, we recorded a ^{1}H-NMR spectrum of **1**. CN^- in DMSO-d_6 after 2 days. The analysis of the spectrum indicated a drastic increase in the number of NMR peaks (Fig. 6d). Thus, it can be concluded that cyanide interaction could lead to the formation of a chemodosimetric adduct in which the chemical environments of the indole moieties are very distinct. The formation of the cyanide adduct was also evident from the detection of the mass spectral peaks of the adducts. Compound **1** with CN^- showed a peak at 939.4081 (calcd mass = 939.4081), which corresponds to the (M–H) of probe **1** (Fig. 6c).

3.5. Detection of endogenous cyanide

In addition to the detection of free cyanide in water, the detection of endogenously bound cyanide ions in many food items is essential. Such foods as cassava are major foods for more than 500 million people in Africa, Asia and Latin

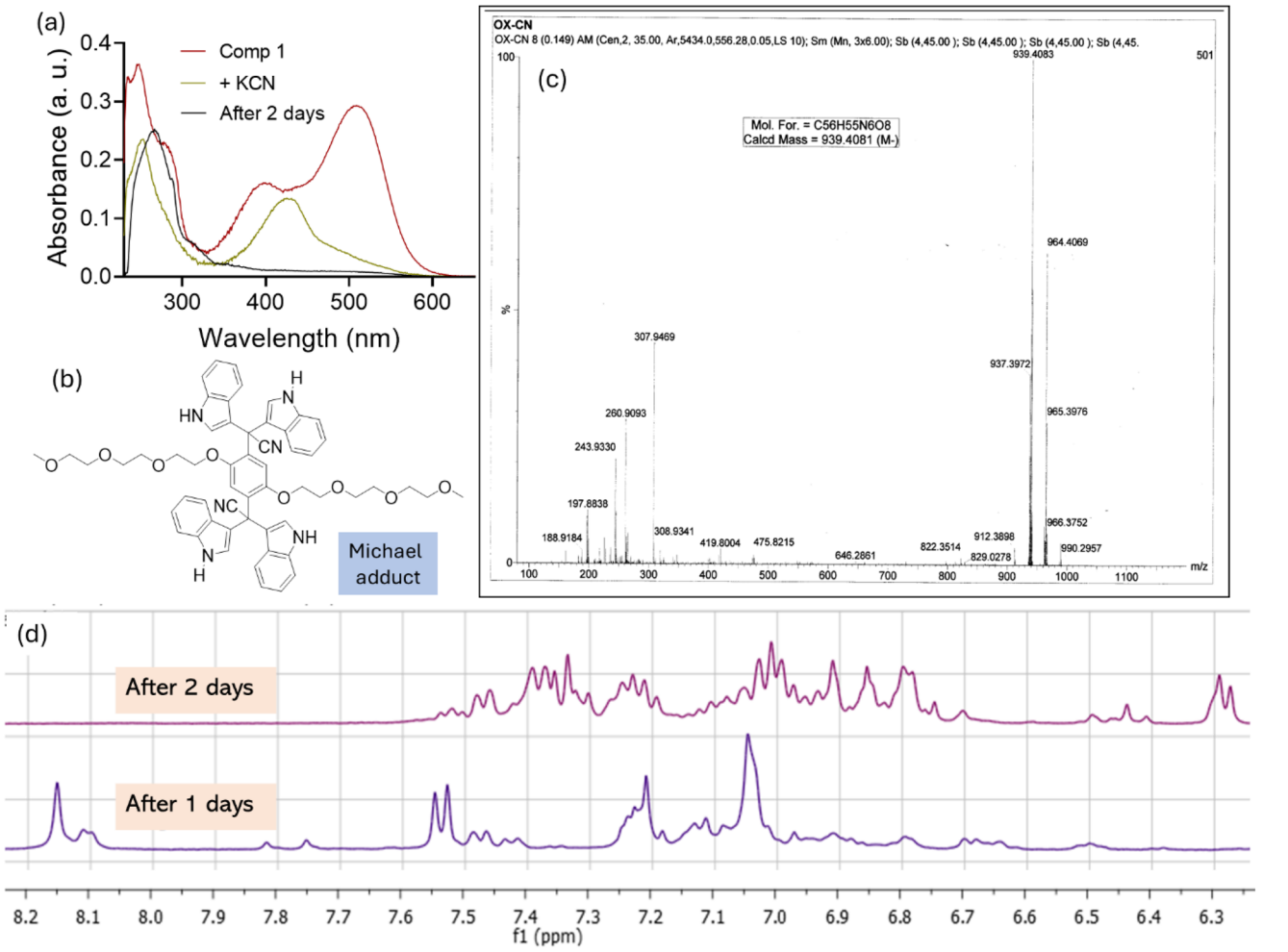

Fig. 6 (a) UV-visible spectra of **1** (10 μM) with CN^-, upon immediate addition and after 2 days. (b) Chemical structure of the chemodosimetric adduct with CN^- ion. (c) HRMS mass spectrum of **1** with CN^- ion after 2 days. (d) Partial ^{1}H-NMR spectra of **1** (5 mM) with CN^- in DMSO-d_6 medium, recorded after 1 and 2 days, respectively.

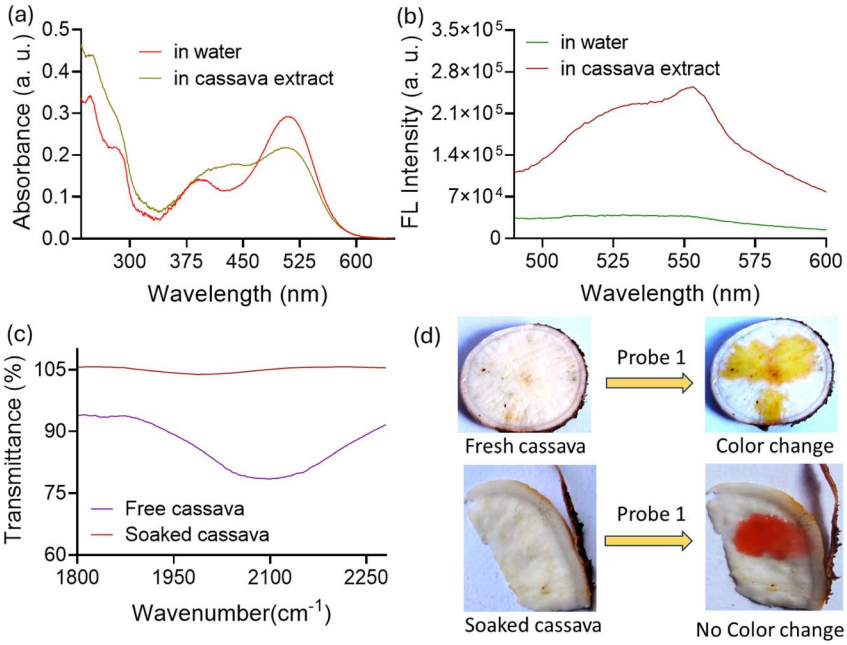

Fig. 7 (a) UV-visible and (b) fluorescence spectra of **1** (20 μM, λ_{ex} = 465 nm) in cassava extract. (c) Partial IR spectra of freshly cut cassava and after keeping it in water for 10 days. (d) Change in the visible color after pouring a few drops of **1** (1 mM) on the cassava slice, both in the freshly cut condition and after keeping it in water for 10 days.

America.[14] Therefore, to determine the utility of the present probe for the detection of endogenous bound cyanide, we used it to detect the presence of cyanide ions in cassava (*Manihot esculenta*). Fresh cassava was procured from the market, and its origin was not specified. To record absorption and fluorescence spectroscopy of cassava soaked in water, we dipped 200 mg of freshly cut cassava slices in 50 mL of water for 30 minutes. The UV-visible spectrum of **1** was recorded in freshly prepared cassava extract (Fig. 7a).[15] A new absorption band was observed 427 nm region, which appeared to be very similar to that observed with KCN in water medium. Furthermore, we recorded the fluorescence spectrum of compound **1** in cassava extract. Furthermore, a turn-on fluorescence response (~6.7 fold) was observed upon 465 nm excitation (Fig. 7b). A similar fluorescence enhancement was observed for KCN in water medium. Therefore, both observations indicate that the cyanide ion released from cassava extract can be detected by compound **1**.

The direct detection of cyanide on cassava slices was performed without any processing. On a freshly cut cassava slice, a few drops of the probe solution (1 mM) were added. A similar color change from red to yellow was observed (Fig. 7d). To determine whether the change was due to complexation with cyanide, we kept a small piece of cassava in water for 10 days.[16] After that, we removed the water and dried the cassava slices at room temperature. When this dried, pretreated cassava slice was spiked with compound **1**, we did not observe any color change. The color of the spot remained red. To confirm whether soaking in water could remove the cyanide ions, we checked the IR spectra of the slices before and after immersion. Compared with freshly cut cassava, it showed the absence of the 2100 cm^{-1} band corresponding to the bound cyanide (Fig. 7c).[17]

4. Conclusion

Herein, we synthesized highly colored, oxidized bis-indolyl derivatives with oligooxyethylene chains as substituents to the central phenyl ring. The incorporation of oxyethylene chains resulted in a significant increase in the solubility of the probe in water. Due to increased solubility, the compound could exert a pronounced response towards cyanide ion, which was reflected in the distinct changes observed in both UV-vis and fluorescence spectroscopic analysis. In addition, such high sensitivity was evident from its exceptionally low detection limit (~17 ppb) for cyanide ions in the aqueous medium. In addition to the naked eye detection, the ratiometric response ensured that this system could significantly reduce background interference, making it highly suitable for quantitative analysis of cyanide ions. The mechanistic investigation revealed a time-dependent two-step interaction between the cyanide ion and the aqueous medium. The first step involved hydrogen bonding (or deprotonation) interactions with cyanide ions involving the acidic indolyl-NH protons, which resulted in an immediate change in the color of the solution from red to yellow. However, upon aging the same solution for a longer duration, we could witness a further change in the color of the solution from yellow to colorless. This result was attributed to a cyanide-triggered Michael addition reaction, which eventually altered the overall conjugation. The formation of the chemodosimetric adduct at a later stage was confirmed by ^{1}H, ^{13}C-NMR, and mass spectral analysis. In addition, the system enables visual detection of endogenous bound cyanide in cassava. The visual response towards cyanide was observed not only in the aqueous extract of the food sample but also when it was directly spiked on the

surface. In addition, we examined whether conventional washing techniques can remove cyanide from cassava samples or not. Such studies will be beneficial not only for the detection of endogenous cyanide in crops but also for developing proper remediation techniques.

Data availability

The data will be available from the corresponding author upon reasonable request.

Conflicts of interest

There are no conflicts to declare.

Acknowledgements

ND thanks DST for SYST grant (grant number: SP/YO/2021/1632). SB thanks IISER Tirupathi and IISD Bangalore for technical facilities and JC Bose fellowship for funding. The authors also thank central analytical facilities BITS Pilani Hyderabad.

References

1 X. He, S. Hu, K. Liu, Y. Guo, J. Xu and S. Shao, Oxidized Bis(indolyl)methane: A Simple and Efficient Chromogenic-Sensing Molecule Based on the Proton Transfer Signaling Mode, *Org. Lett.*, 2006, **8**, 333–336.

2 R. M. N. Kalla and S. C. Hong, I. Kim Synthesis of Bis(indolyl) methanes Using Hyper-Cross-Linked Polyaromatic Spheres Decorated with Bromomethyl Groups as Efficient and Recyclable Catalysts, *ACS Omega*, 2018, **3**, 2242–2253.

3 (*a*) A. Devi, M. M. Bharali, S. Biswas, T. J. Bora, J. K. Nath, S. Lee, Y. B. Park, L. Saikia, M. J. Baruaha and K. K. Bania, Utilization of methanol and ethanol for 3,3′-bis(indolyl) methane synthesis through activation of peroxymonosulfate over a copper catalyst, *Green Chem.*, 2023, **25**, 3443–3448; (*b*) R. S. Fernandes and N. Dey, Metal Ion Responsive Bifunctional Bis(indolyl)methane Derivative: Excitation-Triggered Alteration in the Sensing Behavior, *Mater. Chem. Phys.*, 2023, **302**, 127637.

4 (*a*) A. Srivastava, A. Agarwal, S. K. Gupta and N. Jain, Graphene oxide decorated with Cu(I)Br nanoparticles: a reusable catalyst for the synthesis of potent bis(indolyl) methane based anti-HIV drugs, *RSC Adv.*, 2016, **6**, 23008–23011; (*b*) R. S. Fernandes and N. Dey, Shedding Light on Protein Aggregates by Bisindolyl-Based Fluorogenic Probes: Unveiling Mechanistic Pathways and real-time tracking of protein aggregation, *Biomacromolecules*, 2025, **26**, 1461–1475.

5 (*a*) V. D. Kadu, S. N. Chandrudu, M. G. Hublikar, D. G. Rauta and R. B. Bhosale, Metal-free oxidative coupling of arylmethylamines with indoles: a simple, environmentally benign approach for the synthesis of 3,3′-bis(indolyl) methanes, *RSC Adv.*, 2020, **10**, 23254–23262; (*b*) R. S. Fernandes and N. Dey, Exploring the Synergistic Effect of Aggregation and Hydrogen Bonding: Fluorescent Probe for Dual sensing of Phytic Acid and Uric Acid, *J. Mater. Chem. B*, 2024, **12**, 11789–11799.

6 (*a*) A. Kumar, C. Patel, P. Patil, S. Vyas and A. Sharma, Chemoselective synthesis of bis(indolyl)methanes using sulfonic acid-functionalized chitosan, *Chem. Pap.*, 2019, **73**, 3095–3104; (*b*) R. S. Fernandes and N. Dey, Oxidized bis(indolyl)methane derivatives with Diverse Signaling units: Excitation-Dependent Fluorescence Response Towards Heavy Metal Pollutants in Aqueous Medium, *Ind. Eng. Chem. Res.*, 2023, **62**, 21536–21545.

7 (*a*) A. Pervaiz, S. A. Shahzad, M. A. Assiri, T. Javid, H. Irshad and K. Qvortrup, Cyanide and chloroform detection through J-aggregates based aggregation induced emission probe with real sample applications, *J. Hazard. Mater. Lett.*, 2024, **5**, 100132; (*b*) M. T. Waseem, H. M. Junaid, S. Majeed, A. M. Khan, T. Mahmood and S. A. Shahzad, Fluorene based fluorescent and colorimetric chemosensors for selective detection of cyanide ions in aqueous medium and application of logic gate, *Microchem. J.*, 2022, **173**, 107018; (*c*) J. Jangir, Kiran, A. Ranolia, Priyanka, S. Chahal, S. Singh, A. Duhan, R. K. Dhaka, D. Singh, P. Kumar and J. Sindhu, Colorimetric reversibility: Aqueous phase recognition of cyanide using smart phone-based device with real sample analysis, *Microchem. J.*, 2025, **208**, 112259; (*d*) S. Majeed, M. T. Waseem, H. M. Junaid, G. S. Khan, S. Nawazish, T. Mahmood, A. M. Khan and S. A. Shahzad, Aggregation induced emission-based fluorenes as dual-channel fluorescent probes for rapid detection of cyanide: applications of smartphones and logic gates, *RSC Adv.*, 2022, **12**, 18897–18910; (*e*) S. Majeed, M. T. Waseem, G. S. Khan, H. M. Junaid, M. Imran, S. Nawazish, T. A. Khan, T. Mahmood and S. A. Shahzad, Development of AIEE active fluorescent and colorimetric probe for the solid, solution, and vapor phase detection of cyanide: smartphone and food applications, *Analyst*, 2022, **147**, 3885–3893.

8 (*a*) P. Kamboj and V. Tyagi, Construction of Bis-Indole Derivatives Using α-Amylase Enzyme: Application in the Gram-Scale Synthesis of Bis-Indole Containing Bioactive Molecules, *Asian J. Org. Chem.*, 2023, **12**, e202200669; (*b*) S. Jha, N. Kumari, B. Chettri and N. Dey, Monitoring Local pH of Membranous Aggregates *via* Ratiometric Color Changing Response, *ChemPhysChem*, 2022, **23**, e202200208.

9 (*a*) R. Pegu and S. Pratihar, Colorimetric Sensing of Anions with Bis(indolyl)methane based on Donor Acceptor Interaction: A Study based on Experimental and Computational Evidences, *ChemistrySelect*, 2016, **1**, 3288–3296; (*b*) S. Jha and N. Dey, Differential Chromogenic Response towards F- and H_2PO_4-: Hydrogen Bonding vs Deprotonation, *ChemistrySelect*, 2021, **6**, 9211–9216.

10 S. Jha, N. Kumari, B. Chettri and N. Dey, Monitoring local pH of membranous aggregates *via* ratiometric color changing response, *ChemPhysChem*, 2022, **23**, e202200208.

11 (*a*) S. A. R. Mulla, A. Sudalai, M. Y. Pathan, S. A. Siddique, S. M. Inamdar, S. S. Chavana and R. Santosh Reddy, Efficient, rapid synthesis of bis(indolyl)methane using ethyl ammonium nitrate as an ionic liquid, *RSC Adv.*, 2012,

2, 3525–3529; (*b*) N. Dey, N. Kumari, D. Biswakarma, S. Jha and S. Bhattacharya, Colorimetric Indicators for Specific Recognition of Cu^{2+} and Hg^{2+} in Physiological Media: Effect of Variations of Signaling Unit on Optical Response, *Inorg. Chim. Acta*, 2019, **487**, 50–57.

12 (*a*) N. Kumari, S. Jha and S. Bhattacharya, A Chemodosimetric Probe Based on a Conjugated Oxidized Bis-Indolyl System for Selective Naked-Eye Sensing of Cyanide Ions in Water, *Chem. - Asian J.*, 2012, **7**, 2805–2812; (*b*) R. Pegu, R. Mandal, A. K. Guha and S. Pratihar, A selective ratiometric fluoride ion sensor with a (2,4-dinitrophenyl)hydrazine derivative of bis(indolyl) methane and its mode of interaction, *New J. Chem.*, 2015, **39**, 5984–5990.

13 (*a*) K. Ban, S. Nozaki, T. Aijima, S. Oyama, H. Tsujino, Y. Kanematsu, S. Akai and Y. Sawama, Furanyl bis(indolyl) methane as a palladium ion-selective chromogenic agent, *Org. Biomol. Chem.*, 2024, **22**, 2734–2738; (*b*) N. Kumari, S. Jha and S. Bhattacharya, An Efficient Probe for Rapid Detection of Cyanide in Water at Parts per Billion Levels and Naked-Eye Detection of Endogenous Cyanide, *Chem.–Asian J.*, 2014, **9**, 830–837.

14 S. Paul, R. S. Fernandes and N. Dey, Ppb-Level, Dual Channel Sensing of Cyanide and Bisulfate Ions in Aqueous Medium: Computational Rationalization of Ion-Dependent ICT Mechanism, *New J. Chem.*, 2022, **46**, 18973–18983.

15 R. S. Fernandes and N. Dey, Oxidized bis(indolyl)methane derivatives with Diverse Signaling units: Excitation-Dependent Fluorescence Response Towards Heavy Metal Pollutants in Aqueous Medium, *Ind. Eng. Chem. Res.*, 2023, **62**, 21536–21545.

16 R. Sundaramoorthy, M. Vadivelu, K. Karthikeyan and C. Praveen, Mechanosynthesis of Triazolyl-bis(indolyl) methan Pharmacophores *via* Gold Catalysis: A Prelude to Their Molecular Electronic Properties and Biological Potency, *ChemMedChem*, 2018, **18**, e202200529.

17 H. V. Barkale and N. Dey, Membrane-Bound Bisindolyl-Based Chromogenic Probes: Analysis of Cyanogenic Glycosides in Agricultural Crops for Possible Remediation, *ACS Appl. Bio Mater.*, 2025, **8**, 189–198.